A piecewise-linear adaptive exponential integrate-and-fire neuron model with emerging traveling waves using analytical scheme

A piecewise-linear adaptive exponential integrate-and-fire neuron model with emerging traveling waves using analytical scheme

Chinmay Chakraborty[1], Naresh Saha[2,3], M. A. Aziz-Alaoui[4], Argha Mondal[1,5,⋆], Chris G. Antonopoulos[5], Evgeny P. Zemskov[6]

[1] *Department of Mathematics, Sidho-Kanho-Birsha University, Purulia-723104, WB, India*
[2] *School of Physics, University of Hyderabad, Gachibowli, Hyderabad, 500046, India*
[3] *Department of Mathematics, School of Engineering, Dayananda Sagar University, Bengaluru, 562112, India*
[4] *Normandie Univ, UNIHAVRE, LMAH, FR-CNRS-3335, ISCN, 76600, Le Havre, France*
[5] *School of Mathematics, Statistics and Actuarial Science (SMSAS), University of Essex, Wivenhoe Park, UK*
[6] *FRC CSC RAS, Russian Academy of Sciences, Vavilova 40, 119333 Moscow, Russia*

Abstract

The diverse firing characteristics of the excitable dynamical models are spontaneous organized responses often observed in networks. The adaptive exponential integrate-and-fire (AdEx) model has been widely used to study functional properties in neuronal networks and information processing. The dynamics of piecewise-linear approximation to the AdEx model is explored to enhance mathematical and computational efficiency and accuracy. Analytical calculations and numerical schemes are implemented to solve coupled nonlinear diffusive dynamical equations for traveling wave solutions. More specifically, we explore the diversity among the types of wave we encounter. We determined the approximate solutions using our proposed method and derived the solutions from variations in the diffusion parameters. The traveling front and pulses are explicitly specified and analyzed to validate our analytical scheme. This study contributes to understanding the role of self-diffusion and single cross-diffusion in piecewise linear AdEx models, providing insights into the mechanisms underlying action potential generation. We analyze the effects of different types of diffusion on the model's behavior, including the generation of wave propagation, wave speed, and shape. The findings have implications for modeling neuronal activity, particularly in replicating complex behavior in neuronal computation.

Keywords: AdEx model, Piecewise linear model, Reaction-diffusion system, Traveling waves

1. Introduction

Nonlinear biophysical systems, particularly in neuronal dynamics, generate a rich diversity of spatio-temporal patterns and waves. An important class of waves are excitation traveling waves that propagate in active media without changing their shape and with constant speed [1, 2, 3]. A simple and diverse excitable biophysical model is often required for mathematical and computational simulations of large spiking neuronal networks [4]. The modeling frameworks need to be sufficiently dynamic to cover the complete characteristics of different neurons using a suitable parameter regime. We explore the accountability of a simple two-dimensional model known as the adaptive exponential integrate-and-fire neuron model (AdEx) [5, 6, 7]. The key mechanism of the AdEx model is that it integrates the incoming synaptic input until the membrane potential reaches the threshold. As soon as the threshold is reached, the neuron spikes (generates an action potential) and resets its membrane potential to rest. In addition, the model includes an adaptive mechanism to adjust the threshold based on the history of synaptic inputs. The model exhibits various firing patterns depending on the suitable parameter space [7]. The action potential of a neuron is a brief electrical impulse that allows neurons to transmit information [4, 8, 9]. It's a complex process involving ion channels, pumps, and electrochemical gradients. The electrophysiological states of both cells and axons are distinguished by a reduction in the electric potential across the cellular membrane, which is sustained by the exchange of ions between the intercellular space and the cytoplasm [3, 9, 10].

Computational neuroscience has placed a great deal of emphasis on electrophysiology, ignoring the brain as a complex organ with embedded neuronal networks and the chemophysiology that directly supports neuronal activity [4]. This is

⋆Correspondence
Email addresses: argham@skbu.ac.in

especially crucial as we attempt to modify our models to better understand brain diseases, many of which are linked to variations in the extracellular concentrations of ions, metabolites, transmitters, or toxins in different brain regions [11]. Changes in the extracellular concentration, therefore, lead to modifications in the reactions and reaction rates involving many cellular components, such as intracellular signaling pathways, ion channels, and specific and nonspecific receptors [3, 12]. A non-linear elastic wave propagation mechanism was proposed by a few authors as an explanation for the solitonic qualities of the action potential due to the solitary characteristics of the signals provided by Hodgkin and Huxley [10, 13]. According to these authors, action potential spikes that move against the direction of the axon highlight the possibility that isolated action potential spikes might be annihilated. Solitons, or oscillatory and localized pulse-type solutions, can exist in both space and time for reaction-diffusion (parabolic) equations [9, 14]. Traveling waves in excitable media offer a significant illustration of the self-organization processes in mathematical models and computational approaches for spatially dispersed biological, physical, and chemical systems. The systems of nonlinear reaction-diffusion equations have been extensively studied in biological and biophysical phenomena [15, 16, 17, 18]. Different reaction-diffusion systems have been proposed to study nerve impulse conduction [19, 20, 21, 22]. Analytical results and numerical simulations show that these dynamical equations have traveling front/pulse solutions with various propagation speeds [15, 23, 24]. Spatiotemporal effects in biological excitable systems can be mathematically modeled adequately using dynamical systems [25, 26, 27, 28]. It is often observed that theoretical considerations assume a diagonal diffusion in the reaction-diffusion equations while off-diagonal diffusion is required in some cases [9, 29, 30, 31], especially in neuronal dynamics [19, 32, 33, 34]. The neuron models include membrane voltage dynamics in the first equation, and fronts and other variables are related to the model equations for interactions with the voltage variable. The use of PDEs in studying the neuronal dynamical equations from a dynamical system's perspective is ubiquitous regarding the complexities of biophysical models [21, 32, 35]. Our work aims to determine the existence of traveling fronts and pulses in a neuronal model under a spatial domain. In neuronal dynamics, the impulses that appear in the nerve fibers are represented as traveling waves [19, 20, 36]. The traveling waves are obtained using a system of partial differential equations. The solutions are expressed in $u(x,t) = U(z)$, where $z = x - ct$. The spatial domains are indicated by the variables x and t, c is the wave speed. If $c = 0$, it represents the stationary wave [16, 37].

A two-variable model of spiking neurons is the AdEx model. The activation term in the first equation, having an exponential voltage dependency, explains the membrane potential's dynamics. The second equation that describes adaptation is connected to voltage. If an action potential is triggered, both variables are reset with a suitable parameter regime [5, 7]. The AdEx model employs an exponential function to describe the relationship between membrane potential and spike generation, allowing for a more nuanced and biologically plausible representation of neuronal behavior. In contrast, the piecewise linear (PWL) AdEx model approximates this relationship using a piecewise linear function, which also exhibits some interesting biophysical phenomena and enables the derivation of the analytical solutions for traveling waves-a feature not feasible with the full AdEx model. However, the AdEx model and the corresponding PWL model exhibit several consistent phenomena due to the similar underlying mechanics of both models [5, 7]. One of the primary phenomena consistent in the PWL model is the propagation of action potentials in response to input stimuli, mirroring how biological neurons communicate. Additionally, the PWL model exhibits adaptation, where the neuron adjusts its firing rate based on the input history, allowing it to respond to changing conditions realistically [38, 39]. Traveling waves form a basic class of solutions to reaction-diffusion equations that are mostly used to explain natural phenomena. The key feature of our analytical scheme is that it can determine the speed and shape of the wave by the model parameters, such as the membrane capacitance, conductances, and ion channel kinetics [7]. As neurons communicate with one another through ion channels, we present the concepts of self-diffusion and cross-diffusion. We provide an analytical approach to generate the traveling waves in the spatial domain [24, 36]. We specifically focus on the explanation of some phenomena that often occur in neuronal functioning. We attempt to explain theoretically by introducing diffusion terms with a few scaling parameters on the well-established AdEx model. We investigate the types of traveling wave propagation that can emerge from reaction-diffusion excitable systems of two coupled equations.

In particular, we show the important consequences of the emerging traveling front and pulses in the neuronal system. Due to the nonlinearity that appears in the reaction terms, the construction of the traveling waves solution becomes much more complicated until we adopt the piecewise linear caricature [1, 7, 36, 37]. Naud et al. [7] revealed the importance, along with a comparison with the original model of this caricature, theoretically and provided enough experimental data in support of this. We mainly investigate the self-diffusion effects on the diffusively connected AdEx model. The effect of cross-diffusion has also been investigated [33]. We consider the piecewise linear (PWL) model derived by applying McKean's technique to analytically develop a traveling wave solution [1, 7]. We report that the deterministic model

can produce traveling fronts and pulses under a diffusion-induced situation. The straightforward model is fitted to the characteristics of cortical cell tests with reaction-diffusion systems [40]. The outcomes validate that this type of basic PWL model, like the diffusion-induced AdEx neuron model, is appropriate for extensive network simulations. In this work, we investigate the adaptability and biological significance of the piecewise linear AdEx model.

The paper is organized as follows. We introduce the piecewise linear AdEx model and describe some preliminary ideas for the model with diffusion in Sec. 2. In Sec. 3, we construct the traveling wave solutions and discuss the mathematical details of the general solutions. We summarize our discussion in Sec. 4.

2. An adaptive integrate-and-fire neuron model

The AdEx model equations mimic the evolution of the membrane potential, $V(t)$, and the adaptation current, $w(t)$, when an applied current, I is injected. It was demonstrated to accurately forecast the spike patterns of a conductance-based Hodgkin and Huxley model and other cortical neurons, making it, by design, more realistic than the LIF model [5, 7]. The original model read as follows [7]

$$C\frac{dV}{dt} = -g_L(V - E_L) + g_L\Delta_T \exp\left(\frac{V - V_T}{\Delta_T}\right) + I - w, \tag{1}$$

$$\tau_w \frac{dw}{dt} = a^*(V - E_L) - w. \tag{2}$$

Here, C is the total capacitance, g_L is the total leak conductance, E_L is the effective rest potential, Δ_T is the threshold slope factor, V_T is the effective threshold potential, and τ_w is the time constant. The action potential increases as a result of the exponential term activating positive feedback when the current pushes the potential above $V > 0$. The exponential term is associated with the quasi-instantaneous response of the activation variable related to the sodium channel appearing in the Hodgkin-Huxley type model. The rest threshold is generally set at 0 mV as the upswing gets stopped at this level. A rest condition is introduced in place of the downswing. if $V > 0$ mV then $V \to V_r$, and $w \to w_r = w + b^*$. Here, the voltage reset has a fixed value V_r, and the same for w-reset is b^*. The following bifurcation parameters are mainly proportional to conductance, a^*, time constant τ_w, the spike-triggered adaptation parameter b^*, and V_r. We acquire parameters characterizing the traveling waves by fitting the model using reaction-diffusion equations. Naud et al. [7] applied a piecewise linear approximation (PWL) to this nonlinear model in a manner by McKean [1] and Rinzel–Keller [19] type approach and suggested a caricature with a V-shaped reaction function (kinetic term) in the first equation. PWL models simplify the neuronal behavior into three linear regions: subthreshold, spike, and reset. The PWL methods can effectively capture nonlinear relationships between variables by using multiple linear segments even if the nonlinearities appear in the kinetic term, making them suitable for modeling complex neural dynamics [38, 41].

$$C\frac{dV}{dt} = F(V) - w + I, \tag{3}$$

$$\tau_w \frac{dw}{dt} = a^*(V - E_L) - w, \tag{4}$$

where the nonlinearity in the first equation of the model was replaced by a piecewise linear type function in Eq. 3 [7].

$$F(V) = \begin{cases} -g_L(V - E_L) & \text{if} \quad V \le V_T, \\ g_L\Delta_T(V - E) & \text{otherwise,} \end{cases} \tag{5}$$

with $E = V_T + (V_T - E_L)/\Delta_T$. Such a model with a piecewise linear V-nullcline allows us to solve the reaction-diffusion equations analytically. The evolution of the second system variable, w is changing much slower than the membrane voltage variable, V. We observe that two nullclines of the piecewise model in the (V, w) plane can be obtained analytically [7]. In this article, we can use the result of the piecewise model for the evolution of traveling wave propagation. We focus on the analytical results for the construction of the traveling wave propagation depending on the two system variables. With the function $F(V)$, it is important to describe the system in two cases that depend on the voltage resetting value V_r, which is greater than or less than V_T. We incorporated appropriate parameters while maintaining the V-shape of the nullcline since the V-shape nullcline is required to construct the traveling waves solution in case of piecewise linear

models with diffusion [36]. We introduce the parameters α, β and b in Eqs. $(8)-(9)$ to understand the reaction terms more simply and construct the system of PDEs (Eqs. $(6)-(7)$) using the reaction term $f(u,v)$ and $g(u,v)$. Moving forward, we will refer to the membrane voltage, V, and adaptation variable, w, as u and v, respectively, for the sake of simplicity only. Consequently, the estimated range for α is given by $g_L \leq \alpha \leq g_L\Delta_T$ [7]. The V-shaped nullcline, $f(u,v)=0$ and the linear nullcline $g(u,v)=0$, may intersect at one or two equilibrium points depending on the values of the parameters α and β. The condition $\beta > \alpha$ gives only one point of equilibrium, while the other condition $\beta < \alpha$ provides two equilibrium points (see Fig. 1).

3. Construction of traveling waves in the piecewise linear model

The general two-species reaction-diffusion system includes both self- and cross-diffusion terms [30, 31] for their ability to generate realistic phenomena, and is described by the following equations.

$$\frac{\partial u}{\partial t} = f(u,v) + D_u\frac{\partial^2 u}{\partial x^2} + h_v\frac{\partial^2 v}{\partial x^2}, \tag{6}$$

$$\frac{\partial v}{\partial t} = \varepsilon g(u,v) + D_v\frac{\partial^2 v}{\partial x^2} + h_u\frac{\partial^2 u}{\partial x^2}. \tag{7}$$

The parameter, ε represents the ratio of the time scales and should be positive always. This has led to the adaptation of the AdEx model into a reaction-diffusion framework. The reaction terms $f(u,v)$ and $g(u,v)$ in Eqs. $(6)-(7)$ represent the dynamics of the membrane potential and the adaptation current, respectively, similar to the AdEx model. However, the AdEx model and the reaction-diffusion system represented by Eqs. $(6)-(7)$ share some characteristics, such as traveling wave propagation, wave speed, and wave form, as well as the impact of diffusion on neuronal dynamics [5, 7]. Here, the reaction term in the first equation is the V-shaped function as above

$$f(u,v) = \begin{cases} -\alpha u - v, & u \leq 0, \quad (I) \\ \alpha u - v, & u > 0, \quad (II) \end{cases} \tag{8}$$

and the reaction term in the second equation is a linear function

$$g(u,v) = \beta u - v + b. \tag{9}$$

The model constants α, β, and b have the values for which the system admits the nullclines $f(u,v)=0$ and $g(u,v)=0$ of a V-shape. The V-shaped nullclines with the appropriate parameters are illustrated in Fig. 1. The motivation behind this type of representation is to make the model parameters measurable and biophysically meaningful, which makes it more realistic for studying neuronal activities. The parameter α represents the steepness of the voltage-dependent activation in our piecewise-linear approximation, which corresponds biologically to the sensitivity of ion channel activation during action potential initiation. The parameter β governs the coupling strength between voltage and the adaptation variable, analogous to the influence of applied currents that regulate spike-frequency adaptation. The parameter b defines the spike-triggered adaptation strength, which plays a role in regulating neuronal excitability and firing patterns. The model adapts to various forms of diffusion, including self-diffusion and cross-diffusion, affecting wave propagation, speed, and shape [24, 36]. This makes it well-suited for the study of complex neuronal dynamics. Now, the system (Eqs. $(6)-(7)$) has two nontrivial homogeneous steady states (HSS),

$$(\tilde{u},\tilde{v}) = \left(\frac{-b}{\alpha+\beta}, \frac{\alpha b}{\alpha+\beta}\right), \tag{10}$$

for the first interval and

$$(\tilde{u},\tilde{v}) = \left(\frac{-b}{\beta-\alpha}, \frac{-\alpha b}{\beta-\alpha}\right), \tag{11}$$

for the second interval. Both states are linearly stable steady states of the homogeneous system, i.e., Eqs. $(6)-(7)$ without the spatial term. However, our primary focus is on the pure self-diffusion and pure cross-diffusion cases to simplify the analysis and highlight the fundamental effects of each type of diffusion on the traveling wave solutions. By isolating these cases, we can more clearly demonstrate the distinct impacts of self-diffusion and cross-diffusion on wave propagation, speed, and shape.

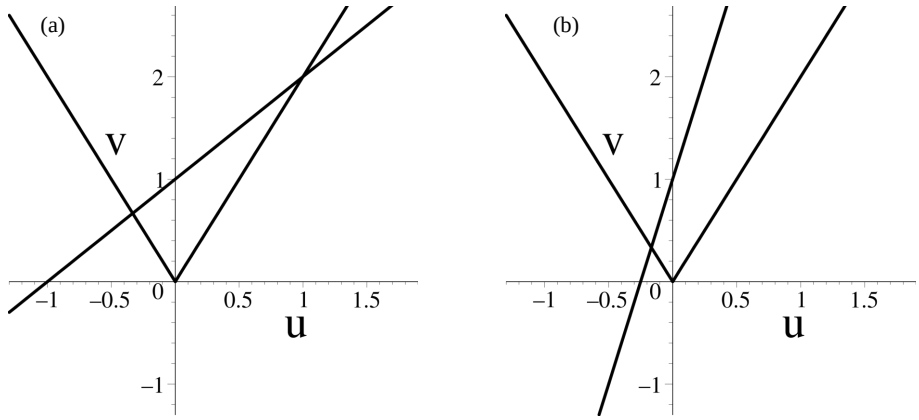

Figure 1: The schematic diagram of nullclines $f(u, v) = 0$ and $g(u, v) = 0$ for Eqs. $(8) - (9)$ with horizontal u-axis and vertical v-axis for different values of α and β.

3.1. Pure self-diffusion case

First, we consider the pure self-diffusion case with $D_u = D_v \equiv D$ and $h_u = h_v = 0$, the self-diffusion coefficient in a neuron model represents the rate at which molecules move randomly within the neuron. Here, D represents the effective diffusivity of membrane potential and recovery variables, which indirectly capture ion flux dynamics during action potential generation. This assumption describes a situation where the diffusion processes for the membrane potential and the adaptation current are uniform and occur at the same rate [36]. This simplification allows for understanding the effects of diffusion. Changes in the self-diffusion coefficient can significantly impact the neuron model's behavior and functionality. Self-diffusion plays a role in the propagation of action potentials along the axon by facilitating the movement of ions and molecules that contribute to the generation and maintenance of the action potential [20, 23, 32]. It also contributes to the removal of waste products and the maintenance of proper ionic balance within the neuron, i.e., the model equations read as follows

$$\frac{\partial u}{\partial t} = f(u, v) + D\frac{\partial^2 u}{\partial x^2}, \tag{12}$$

$$\frac{\partial v}{\partial t} = \varepsilon g(u, v) + D\frac{\partial^2 v}{\partial x^2}. \tag{13}$$

Here, we are looking for traveling wave solutions for these reaction-diffusion equations. The traveling waves propagate in space without change of the wave shape and with constant speed. A traveling pulse is a homoclinic connection that climbs to values close to the second nontrivial HSS after departing from the first nontrivial HSS and then returns to it [30]. The traveling wave solutions are $u = u(\xi)$ and $v = v(\xi)$, where $\xi = x - ct$ is the traveling wave coordinate and c is the propagation speed, i.e., these solutions satisfy ODEs

$$D\frac{d^2 u}{d\xi^2} + c\frac{du}{d\xi} + f(u, v) = 0, \tag{14}$$

$$D\frac{d^2 v}{d\xi^2} + c\frac{dv}{d\xi} + \varepsilon g(u, v) = 0. \tag{15}$$

As the system $(14) - (15)$ is linear, the solutions are linear combinations of exponential functions. We try to find these solutions in the form

$$u(\xi) = \sum_{n=1}^{4} A_n e^{\lambda_n \xi} + u^*, \tag{16}$$

$$v(\xi) = \sum_{n=1}^{4} B_n e^{\lambda_n \xi} + v^*, \tag{17}$$

where A_n, B_n are constants u^* and v^* are HSS respectively. Inserting these solutions into the above Eqs. $(14) - (15)$

and collecting the like terms, we obtain the following matrix equations

$$\begin{pmatrix} D\lambda^2+c\lambda-\alpha & -1 \\ \varepsilon\beta & D\lambda^2+c\lambda-\varepsilon \end{pmatrix}\begin{pmatrix} A \\ B \end{pmatrix}=0, \tag{18}$$

for the first interval and

$$\begin{pmatrix} D\lambda^2+c\lambda+\alpha & -1 \\ \varepsilon\beta & D\lambda^2+c\lambda-\varepsilon \end{pmatrix}\begin{pmatrix} A \\ B \end{pmatrix}=0, \tag{19}$$

for the second interval. For simplicity, we remove the subscript n and write A, B and λ in place of A_n, B_n and λ_n respectively. Now, we can write the characteristic equations

$$(D\lambda^2+c\lambda-\alpha)(D\lambda^2+c\lambda-\varepsilon)+\varepsilon\beta=0, \tag{20}$$
$$(D\lambda^2+c\lambda+\alpha)(D\lambda^2+c\lambda-\varepsilon)+\varepsilon\beta=0, \tag{21}$$

for the first and second intervals, respectively. The characteristic equations have the roots (the eigenvalues):

$$\lambda_{1,2n}=k_{1,2}^{\pm}\pm il_{1,2},\quad n=1,2,3,4, \tag{22}$$

where $k_{1,2}^{+,-}=-m\pm k_{1,2}$, $m=\frac{c}{2D}$, $k_{1,2}=\sqrt{\frac{\sqrt{\left(m^2+\frac{P_{1,2}}{D}\right)^2+\left(\frac{q_{1,2}}{D}\right)^2}+\left(m^2+\frac{P_{1,2}}{D}\right)}{2}}$, $l_{1,2}=\sqrt{\frac{\sqrt{\left(m^2+\frac{P_{1,2}}{D}\right)^2+\left(\frac{q_{1,2}}{D}\right)^2}-\left(m^2+\frac{P_{1,2}}{D}\right)}{2}}$, $p_{1,2}=\frac{\varepsilon\pm\alpha}{2}$, $q_{1,2}=\sqrt{\varepsilon(\beta\pm\alpha)-(\frac{\varepsilon\pm\alpha}{2})^2}$.

Thus, we obtain the general solutions for the traveling waves as

$$u(\xi)=A_1e^{\lambda_1\xi}+A_2e^{\lambda_2\xi}+A_3e^{\lambda_3\xi}+A_4e^{\lambda_4\xi}+u^*, \tag{23}$$
$$v(\xi)=B_1e^{\lambda_1\xi}+B_2e^{\lambda_2\xi}+B_3e^{\lambda_3\xi}+B_4e^{\lambda_4\xi}+v^*, \tag{24}$$

where the integration constants B are given by the expressions as follows

$$B_{n1,3}=-\frac{\varepsilon\beta\left(\delta_{1,2}^{+}A_{n1,3}\mp\theta_{1,2}^{+}A_{n3,1}\right)}{\left(\delta_{1,2}^{+}\right)^2+\left(\theta_{1,2}^{+}\right)^2},\quad n=1,2 \tag{25}$$

$$B_{n2,4}=-\frac{\varepsilon\beta\left(\delta_{1,2}^{-}A_{n2,4}\mp\theta_{1,2}^{-}A_{n4,2}\right)}{\left(\delta_{1,2}^{-}\right)^2+\left(\theta_{1,2}^{-}\right)^2},\quad n=1,2 \tag{26}$$

where

$$\delta_{1,2}^{+,-}=D((k_{1,2}^{+,-})^2-l_{1,2}^2)+ck_{1,2}^{+,-}-\varepsilon,$$
$$\theta_{1,2}^{+,-}=2Dk_{1,2}^{+,-}l_{1,2}+cl_{1,2}.$$

The pulse solutions in such a piecewise linear model consist of three parts, $u_{1,2,3}$ and $v_{1,2,3}$, for the first and second variables, respectively. As $\xi\to\pm\infty$, the pulse approaches a constant value. Thus, the pulse solutions read [16, 36]

$$u_1(\xi)=e^{k_1^{+}\xi}[A_{11}cos\,(l_1\xi)+A_{13}sin\,(l_1\xi)]-b/(\alpha+\beta), \tag{27}$$
$$u_2(\xi)=e^{k_2^{+}\xi}[A_{21}cos\,(l_2\xi)+A_{23}sin\,(l_2\xi)]+e^{k_2^{-}\xi}[A_{22}cos\,(l_2\xi)+A_{24}sin\,(l_2\xi)]-b/(\beta-\alpha), \tag{28}$$
$$u_3(\xi)=e^{k_1^{-}\xi}[A_{12}cos\,(l_1\xi)+A_{14}sin\,(l_1\xi)]-b/(\alpha+\beta), \tag{29}$$

for the first variable and

$$v_1(\xi)=e^{k_1^{+}\xi}[B_{11}cos\,(l_1\xi)+B_{13}sin\,(l_1\xi)]+\alpha b/(\alpha+\beta), \tag{30}$$
$$v_2(\xi)=e^{k_2^{+}\xi}[B_{21}cos\,(l_2\xi)+B_{23}sin\,(l_2\xi)]+e^{k_2^{-}\xi}[B_{22}cos\,(l_2\xi)+B_{24}sin\,(l_2\xi)]-\alpha b/(\beta-\alpha), \tag{31}$$
$$v_3(\xi)=e^{k_1^{-}\xi}[B_{12}cos\,(l_1\xi)+B_{14}sin\,(l_1\xi)]+\alpha b/(\alpha+\beta), \tag{32}$$

for the second variable. The middle parts, u_2 and v_2, correspond to the peaks of the pulses, whereas the edge parts, or tails, u_1, v_1, and u_3, v_3, represent the growing and decaying parts, respectively (the superscripts denote the first and second intervals). The three parts of the pulse profile are fitted together using a specific matching procedure. The matching conditions for the pieces $u_n(\xi)$, $v_n(\xi)$ $n = 1, 2, 3$ and their derivatives $\frac{du_n}{d\xi}, \frac{dv_n}{d\xi}$ at the two matching points $\xi = \xi_0$ and $\xi = \xi_0^*$, are as follows,

$$u_1(\xi_0) = u_2(\xi_0), \frac{du_1(\xi_0)}{d\xi} = \frac{du_2(\xi_0)}{d\xi}, \tag{33}$$

$$u_2(\xi_0^*) = u_3(\xi_0^*), \frac{du_2(\xi_0^*)}{d\xi} = \frac{du_3(\xi_0^*)}{d\xi}, \tag{34}$$

$$v_1(\xi_0) = v_2(\xi_0), \frac{dv_1(\xi_0)}{d\xi} = \frac{dv_2(\xi_0)}{d\xi}, \tag{35}$$

$$v_2(\xi_0^*) = v_3(\xi_0^*), \frac{dv_2(\xi_0^*)}{d\xi} = \frac{dv_3(\xi_0^*)}{d\xi}. \tag{36}$$

We know the value of $u(\xi)$ at the matching points and obtain two additional equations,

$$u_1(\xi_0) = u_3(\xi_0^*) = a. \tag{37}$$

In total, we have ten equations for ten unknown constants, $(A_{11}, A_{12}, A_{13}, A_{14}, A_{21}, A_{22}, A_{23}, A_{24}, \xi_0^*, c)$ which allows us to determine the front speed c and the second matching point ξ_0^* uniquely [30, 36]. The first matching point ξ_0 is chosen to be zero due to the translation invariance of the equations. The parameter a denote the values of $u(\xi)$ at two matching points. Biologically, the parameter a represents the subthreshold adaptation strength, analogous to the activity of voltage-gated channels that regulate resting membrane stability. The presence of traveling pulse solutions in a neuron model is a fundamental aspect of neuronal functioning and has significant implications for our understanding of brain function, behavior, and neuronal disorders [16, 33, 35]. If a neuron model admits traveling pulse solutions, it means that the model can generate and propagate localized wave-like solutions, such as action potentials or spikes, that travel along the axon [8, 12]. There are some parameter sets, we reported in this article, for which the PWL model admits a solitary pulse solution and forms a homoclinic orbit in the (u, v) phase diagram.

The results of the analytical calculations for Eqs. (12) − (13) with $f(u, v)$ and $g(u, v)$ given by Eqs. (8) − (9) and solitary pulses are illustrated in Fig. 2 for pure self diffusion case. We locate the parameters first as we attempt to develop the traveling wave solution. Primarily, we starts with $D = 0.7692$ and adjust other parameters at $a = 0.98$, $\varepsilon = 0.3009$, $\alpha = 4.2871$, $\beta = 21.86$, $b = -12.06$, $\xi_0^* = 1.9$. We observe that the traveling pulse propagates and forms a homoclinic orbit in the (u, v) phase plane at this point on the parameter space (see Figs. $2(a), (d)$). The computed wave speed $c \approx 1.3425$ matches well with the known range of action potential propagation velocity [30, 36]. We then set $D = 0.78$ and leave the other settings at $a = 1.5$, $\varepsilon = 0.23$, $\alpha = 5.67$, $\beta = 66.90$, $b = -62.37$, $\xi_0^* = 3.1$. Next, we fix $D = 0.912$ leaving the other parameters at $a = 2.8$, $\varepsilon = 0.316$, $\alpha = 9.723$, $\beta = 113.62$, $b = -166.64$, $\xi_0^* = 1.5$. In each of these scenarios, a traveling wave propagates, and the computed wave speed $c \approx 3.578$ and $c \approx 2.913$, respectively, agree nicely (see Figs. $2(b), (c)$). Note that, the nullclines intersect at a single equilibrium point and the solutions produce homoclinic orbit in the (u, v)-plane under all such conditions, we mention (see Figs. $2(e), (f)$).

Our numerical experiment contextually illustrates that an increment in the diffusion coefficient leads to a faster propagation speed of action potentials in neurons. This is because the diffusion coefficient represents how easily ions can diffuse across the cell membrane, and a higher value means that ions can move more quickly, resulting in faster signal transmission [42]. However, the values of D greater than one could be an artifact and may not reflect realistic phenomena; we dare to explore numerically. We fix D to 1, 1.1, along with the appropriate tuning of other parameters at $a = 0.5$, $\varepsilon = 0.1$, $D = 1.1$, $b = -3.52$, $\alpha = 0.1$, $\beta = 7.26$, $\xi_0^* = 5$ and $a = 0.1$, $\varepsilon = 0.1$, $D = 1$, $b = -0.496$, $\alpha = 0.4$, $\beta = 5.46$, $\xi_0^* = 8$ respectively. We observed a slow-fast wave in this case (see Figs. $3(a), (b)$).

The dynamics of slow-fast waves are crucial in understanding information processing, neuronal synchronization, and rhythm generation in neurons [43]. However, these types of waves in a diffusive neuron model can be understood by considering the interactions between the slow and fast wave components. Slow waves are generated by the gradual changes in membrane potential whereas, fast waves are generated by the rapid activation of sodium channels. Different types of complex wave patterns can be produced due to the collision of slow and fast waves [44]. The calculated wave speeds $c \approx 1.5$ and 1.9, respectively, fit nicely. A dispersive wave is a traveling wave that spreads out or disperses as it

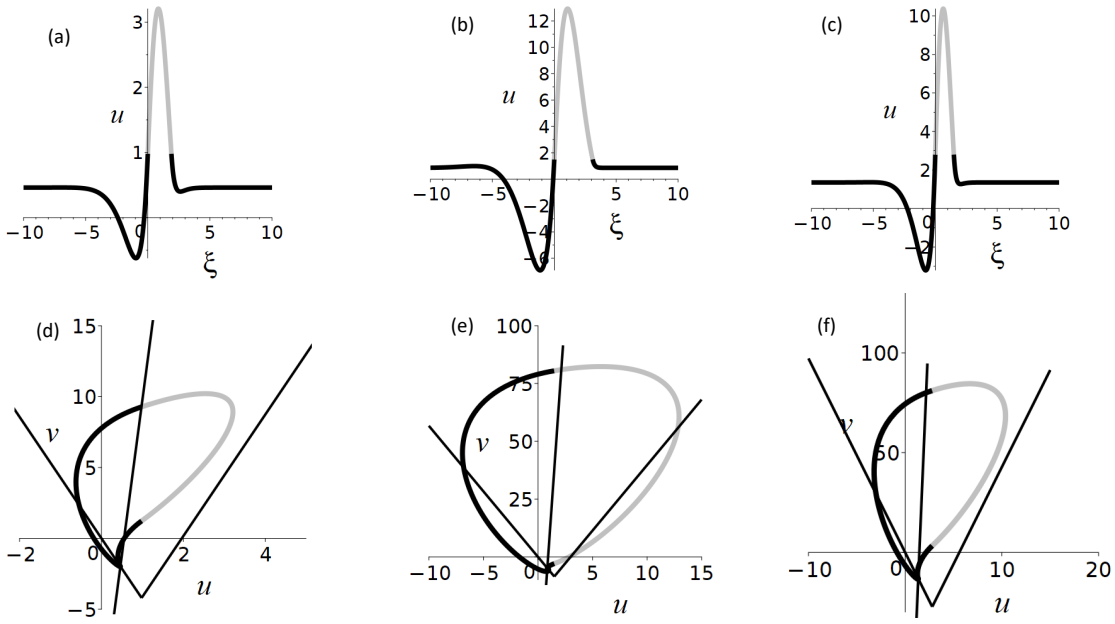

Figure 2: Numerical results of the analytical derivation for traveling pulse solutions with pure self-diffusion, $D_u = D_v \equiv D$ at $D = 0.7692, 0.78$ and 0.912, respectively. The pulse profiles for the spatial variable $u(\xi)$ $[(a), (b), (c)]$ and the trajectories in the $(u, v)-$phase plane $[(d), (e), (f)]$ are shown. The nullclines $f(u, v) = 0$ and $g(u, v) = 0$ are shown in the panels $[(d), (e), (f)]$. However, the nullclines shifted from the origin as we use the form $f(u, v) = \alpha u - v - a = 0$, $(a > 0)$, for the second component of the nullcline.

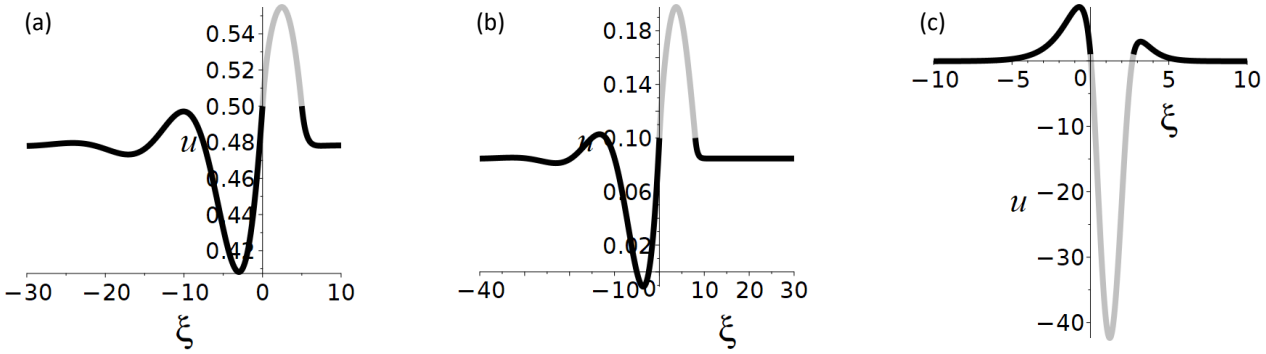

Figure 3: The traveling pulse profiles $u(\xi)$ $[(a), (b), (c)]$ with the self-diffusion case, $D_u = D_v \equiv D$ at $D = 1.1, 1$ and 1.2 are shown.

propagates, often observed in systems with dispersion relations. The dynamics of an inverted pulse refers to the behavior of a pulse that has a reversed polarity compared to a typical action potential [36]. Inverted pulses can occur in certain types of neurons or under specific conditions. The dynamics of inverted pulses in neuron models may provide insights into the mechanisms underlying various functions. An inverted pulse also has been observed in our parameter space $a = 1$, $\varepsilon = 0.4$, $D = 1.2$, $b = 1$, $\alpha = 6.57$, $\beta = 14$, $c \approx 0.629$, $\xi_0^* = 2.75$ (Fig. $3(c)$). An inverted pulse refers to a brief, rapid decrease in the membrane potential of a neuron, often in response to an inhibitory input [12]. This decrease in potential is opposite in direction to the typical excitatory response, where the membrane potential increases.

3.2. Pure cross-diffusion case

Now, we consider the pure cross-diffusion case with a single cross-diffusion term in the first equation when $D_u = D_v = 0$, $h_u = 0, h_v \equiv h$, and $\varepsilon = 1$. Cross-diffusion, a phenomenon where the movement of one species affects the movement of another, has been increasingly recognized as a crucial aspect of neuronal communication. The cross-diffusion coefficient h is a critical parameter in diffusively induced neuron models, as it significantly impacts various aspects of neuronal functioning. Here, the cross-diffusion coefficient h represents the influence of the adaptation current v on the spatial

spread of the membrane potential u, modeling how ion concentration gradients or regulatory mechanisms in neurons can indirectly shape action potential propagation. Biologically, it describes the non-local interactions of ions in neuron membranes. Note that the models with cross-diffusion, but for which self-diffusion disappears, can be complicated to study mathematically, as such situations lead to a lack of L^2 estimates for u and v. However, this gap can be filled as proposed in [29]. It is also interesting to note that the occurrence of bifurcations (like Turing bifurcation) is influenced by the variation of cross-diffusion coefficients, so the case without self-diffusion has a strong impact on these bifurcation phenomena (for more information, see also [45]). Recently, single cross-diffusion has been highly used to boost neuronal responses, decrease synchronization error, and improve spike timing accuracy [16, 30]. The cross-diffusion coefficient represents the rate at which ions or molecules move across the neuronal membrane, influencing the neuron's behavior [42]. Here, we use the concept of single cross-diffusion across the neuron membrane. There are also some physiological aspects, as the equation describes how ions diffuse across the cell membrane, driven by concentration gradients and the permeability of the membrane. This model is described by the PDEs

$$\frac{\partial u}{\partial t} = f(u,v) + h\frac{\partial^2 v}{\partial x^2}, \tag{38}$$

$$\frac{\partial v}{\partial t} = g(u,v). \tag{39}$$

The reaction functions are the same as above. The corresponding ODEs are

$$h\frac{d^2 v}{d\xi^2} + c\frac{du}{d\xi} + f(u,v) = 0, \tag{40}$$

$$c\frac{dv}{d\xi} + g(u,v) = 0. \tag{41}$$

Now, the matrix equations become

$$\begin{pmatrix} c\lambda - \alpha & h\lambda^2 - 1 \\ \beta & c\lambda - 1 \end{pmatrix} \begin{pmatrix} A \\ B \end{pmatrix} = 0, \tag{42}$$

for the first interval and

$$\begin{pmatrix} c\lambda + \alpha & h\lambda^2 - 1 \\ \beta & c\lambda - 1 \end{pmatrix} \begin{pmatrix} A \\ B \end{pmatrix} = 0, \tag{43}$$

for the second interval. Hence, we have the characteristic equations

$$(c\lambda - \alpha)(c\lambda - 1) - \beta(h\lambda^2 - 1) = 0, \tag{44}$$

$$(c\lambda + \alpha)(c\lambda - 1) - \beta(h\lambda^2 - 1) = 0, \tag{45}$$

for the first and second intervals, respectively. The eigenvalues are

$$\lambda_{1,2} = a_1 \pm ib_1, \tag{46}$$

$$\lambda_{3,4} = a_2 \pm ib_2, \tag{47}$$

for the first and second intervals, respectively, where

$$a_1 = \frac{-c(1+\alpha)}{2(\beta h - c^2)}, \tag{48}$$

$$b_1 = \frac{\sqrt{4(c^2-\beta h)(\beta+\alpha) - c^2(1+\alpha)^2}}{2(\beta h - c^2)}, \tag{49}$$

$$a_2 = \frac{-c(1-\alpha)}{2(\beta h - c^2)}, \tag{50}$$

$$b_2 = \frac{\sqrt{4(c^2-\beta h)(\beta-\alpha) - c^2(1-\alpha)^2}}{2(\beta h - c^2)}. \tag{51}$$

The integration constants are

$$B_{1,2} = \frac{\beta(1+ca_1)A_{1,2} \mp cb_1 A_{2,1}}{(1+ca_1)^2 + (cb_1)^2}, \tag{52}$$

$$B_{3,4} = \frac{\beta(1+ca_2)A_{3,4} \mp cb_2 A_{4,3}}{(1+ca_2)^2 + (cb_2)^2}. \tag{53}$$

Thus, the traveling wave solutions read as follows

$$u_1(\xi) = e^{a_1\xi}(A_1 cos(b_1\xi) + A_2 sin(b_1\xi)) - \frac{b}{\alpha+\beta}, \tag{54}$$

$$u_2(\xi) = e^{a_2\xi}(A_3 cos(b_2\xi) + A_4 sin(b_2\xi)) - \frac{b}{\beta-\alpha}, \tag{55}$$

for the first variable and

$$v_1(\xi) = e^{a_1\xi}(B_1 cos(b_1\xi) + B_2 sin(b_1\xi)) + \frac{\alpha b}{\alpha+\beta}, \tag{56}$$

$$v_2(\xi) = e^{a_2\xi}(B_3 cos(b_2\xi) + B_4 sin(b_2\xi)) - \frac{\alpha b}{\beta-\alpha}, \tag{57}$$

for the second variable. Using continuity of the solutions, we obtain [30]

$$u_1(\xi_0) = a, u_2(\xi_0) = a, \frac{du_1(\xi_0)}{d\xi} = \frac{du_2(\xi_0)}{d\xi}, \tag{58}$$

$$v_1(\xi_0) = v_2(\xi_0), \frac{dv_1(\xi_0)}{d\xi} = \frac{dv_2(\xi_0)}{d\xi}. \tag{59}$$

To find the wave profiles, we obtain five equations with five unknown variables A_1, A_2, A_3, A_4, c, which enable us to find the value of c. The findings of these analytical calculations are illustrated in Fig. 4. The existence of the solitary pulse (see Fig. 4(a)) has been confirmed for the cross-diffused model. We explored different parameter sets to confirm the co-existence of the solitary pulse as well as fronts (Fig. 4). Since the propagation of an action potential involves a biochemical process, we are incapable of altering one parameter while maintaining the stability of the other. Consequently, we must modify other parameters as well as to verify the influence of varying cross-diffusion coefficients. We consider the initial value $h = 0.01$ with the other parameters at $a = 0.3$, $\alpha = 1.8$, $\beta = 5.8$ and $b = 0.5$. We observe that a solitary pulse propagates at an uninterrupted pace and without changing shape (see Fig. 4(a)). The wave speed, $c \approx 0.332$, agrees well with the analytical calculations [36, 46].

Additionally, the solution creates a homoclinic orbit in the (u, v)-plane (Fig. 4(d)). Then, a little increase in the diffusion coefficient has been implemented to observe the outcome. Therefore, we set $h = 0.05$ and tune the other parameters at $a = 0.3$, $\alpha = 1.9$, $\beta = 3.5$ and $b = 0.5$. This time, the front with peaks, normal and inverted, is observed (see Fig. 4(b)) and it has its significance [8]. Next, we fix $h = 0.1$, leaving the others parameters at $a = 1.5$, $\alpha = 1.8$, $\beta = 2.5$ and $b = 1.5$. A similar kind of front (Fig. 4(c)) is observed this time as well. Both the time and the calculated wave speed, $c \approx 1.441$ and $c \approx 2.207$, respectively, are in a reasonable range. In all scenarios, the solutions generate a

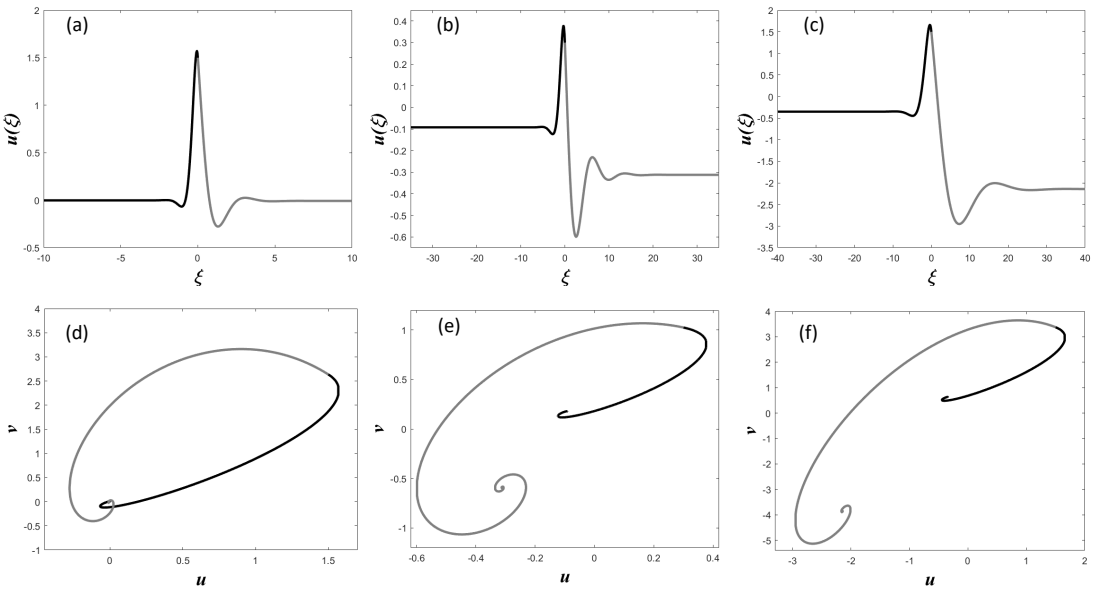

Figure 4: Numerical results of the analytical derivation for traveling front and pulses $u(\xi)$ $[(a),(b),(c)]$ with single cross-diffusion, $h_u = 0$, $h_v \equiv h$, at $h = 0.01, 0.05$ and 0.1 are shown. The corresponding phase diagram in the (u, v)-plane are shown in the panel $[(d),(e),(f)]$

heteroclinic orbit in the (u, v)-plane (see Figs. $4(e),(f)$) [47]. Thus, we observe the transformation from the traveling pulses to fronts as the orbit changes from the homoclinic to the heteroclinic in the phase space. Our computational analysis unambiguously shows that an increase in the cross-diffusion coefficient accelerates the propagation of the action potential. We noticed that a single cross-diffusion connection is more efficient in generating an action potential than the self-diffusion connection under a favorable parameter regime. As we increased the single cross-diffusion coefficient h from 0.01 to 0.1, a drastic increment in the wave speed was observed. This particular parameter set, which we reported here, shows that the single cross-diffusion coefficient regulates the rate of diffusion based on the membrane potential. When the membrane potential is high, the diffusion coefficient increases, allowing more ions to diffuse across the membrane [32, 33, 47].

4. Discussion and conclusions

In this section, we highlighted the primary outcomes of our study in the excitable reaction-diffusion system. We can precisely solve the model equations analytically, construct traveling wave profiles, and as certain the wave speed in the piecewise linear model. It can take a straightforward and adaptable single-neuron modeling framework to simulate massive spiking neuron networks. Here, we investigate the adaptability of the two-dimensional excitable PWL AdEx model. Our results demonstrate that the PWL approximation faithfully reproduces qualitative behavior i.e., pulse shapes, speed ranges observed in AdEx simulations, validating its utility as a tool for probing excitable systems [48]. The dynamics are characterized by the occurrence of fronts and pulses. This approach applies to a broad class of two-variable reaction-diffusion systems. A fundamental class of solutions to the reaction-diffusion equation is made up of traveling waves, which are primarily used to explain natural occurrences [8, 49]. This wave specifically describes the spatiotemporal evolution of the membrane potential. In a range of two-dimensional nonlinear biophysical systems, this kind of wave propagation may result in the production of intricate patterns. The model has gained a lot of attention in the field of computational neuroscience since its parameters are quantifiable and biophysically significant. The damping behavior of the oscillating tails is under consideration apart from conventional periodic waves, which are essential solutions of oscillatory reaction-diffusion equations [18, 30, 36]. This study has investigated the dynamics of diffusion and traveling waves in piecewise linear neuron models, providing valuable insights into the complex behavior of neuronal networks [30, 32]. The analysis revealed that the piecewise linear structure allows for the coexistence of different wave types, including traveling fronts and pulses, and that the model's parameters significantly influence wave propagation speeds and stability [21, 36]. Overall, the PWL model provides a powerful framework for simulating and analyzing the behavior

of neural networks, and its ability to replicate a wide range of phenomena that are consistent with Adex model makes it helpful in understanding the complex dynamics of neurons.

Our investigation seeks to demonstrate the impact of varying the self and cross-diffusion coefficients on the emerging traveling waves. The diffusion coefficients have a significant impact on the movement of ions, which can affect the generation and characteristics of action potentials. A small change in the diffusion coefficient can alter the excitabilities and wave propagation of neurons. We observe the changes in the wave speed as the diffusion coefficient varies. Our solution for the pure self-diffusion and single cross-diffusion cases shows the existence of stationary traveling pulses and fronts, indicating the regenerative nature of action potential propagation, where the depolarization of one neuron segment triggers the depolarization of adjacent segments. This study investigates traveling wave solutions in a diffusion-induced piecewise linear AdEx model, providing a comprehensive understanding of the model's dynamics. We can establish the existence of traveling wave solutions, representing the propagation of fronts and pulses as a result of certain neuronal activities [9, 11, 33, 35]. Our analytical solutions yield wave speed, c, that align with experimentally measured action potential velocities in axons, as well as in cortical and invertebrate neurons where slower propagation is common [13]. The wave shapes (e.g., pulses, fronts, and inverted pulses) reflect known spiking and refractory dynamics, with the homoclinic and heteroclinic orbits in our phase-space analysis corresponding to depolarization-repolarization cycles observed in electrophysiological studies [12, 48]. Future work will explicitly map model parameters to biophysical properties to refine quantitative comparisons. Furthermore, our findings indicate that diffusion plays a crucial role in regulating wave dynamics, enabling or suppressing wave propagation depending on the specific parameter regime. These results contribute to the ongoing efforts to understand the intricate mechanisms governing neural information processing and have implications for developing more realistic models of neuronal networks. This approach explores the relationship between the characteristics of traveling-pulse and seizure dynamics, showing that such perturbations can measure neural excitability and resilience. Analyzing evoked responses revealed an inverse correlation between recovery rates and excitability levels [50, 51]. Studying diffusion parameters governing wave speed and shape may identify therapeutic targets, like ion channel modulation, to disrupt harmful activity, bridging biophysical mechanisms and theoretical behavior for precision therapies. Our piecewise-linear AdEx model generates traveling waves like Wilson-Cowan equations but focuses on single-neuron biophysics, not population-level dynamics [52]. Unlike Kuramoto oscillators, our waves arise from nonlinear spiking and diffusive coupling. This approach balances biological specificity with analytical tractability, providing direct links to measurable neuronal parameters.

Future research directions may include exploring the effects of nonlinearities, heterogeneity, and stochasticity on wave dynamics in piecewise linear neuron models, as well as investigating the relationship between wave propagation and cognitive functions. Overall, this study highlights the importance of mathematical modeling in neuroscience and demonstrates the potential of piecewise linear models to capture essential features of neuronal dynamics, paving the way for a deeper understanding of the complex phenomena underlying brain function.

Acknowledgement

This work is supported by the National Board for Higher Mathematics (NBHM), India, Department of Atomic Energy, Govt. of India under Grant No. 02011/11/2022NBHM(R.P)/R & D-II/10217 to the author Argha Mondal. N. Saha acknowledges IOE-UOH for the financial support through the IOE-PDRF scheme.

Data availability

All numerically simulated data generated or analyzed during this study are included in this submitted article.

Declaration of Competing Interest

The authors declare that they have no known competing financial interests or personal relationships that could have appeared to influence the work reported in this paper.

References

[1] H. P. McKean Jr, Nagumo's equation, Advances in mathematics 4 (3) (1970) 209–223.

[2] S. Hastings, On the existence of homoclinic and periodic orbits for the FitzHugh-Nagumo equations, The Quarterly Journal of Mathematics 27 (1) (1976) 123–134.

[3] R. Phillips, J. Kondev, J. Theriot, H. Garcia, Physical biology of the cell, Garland Science, 2012.

[4] E. M. Izhikevich, Dynamical systems in neuroscience, MIT press, 2007.

[5] R. Brette, W. Gerstner, Adaptive exponential integrate-and-fire model as an effective description of neuronal activity, Journal of neurophysiology 94 (5) (2005) 3637–3642.

[6] C. Clopath, R. Jolivet, A. Rauch, H.-R. Lüscher, W. Gerstner, Predicting neuronal activity with simple models of the threshold type: Adaptive exponential integrate-and-fire model with two compartments, Neurocomputing 70 (10-12) (2007) 1668–1673.

[7] R. Naud, N. Marcille, C. Clopath, W. Gerstner, Firing patterns in the adaptive exponential integrate-and-fire model, Biological cybernetics 99 (2008) 335–347.

[8] J. Nagumo, S. Arimoto, S. Yoshizawa, An active pulse transmission line simulating nerve axon, Proceedings of the IRE 50 (10) (1962) 2061–2070.

[9] G. Cano, R. Dilão, Action potential solitons and waves in axons, Chaos, Solitons & Fractals 178 (2024) 114335.

[10] T. Heimburg, A. D. Jackson, On soliton propagation in biomembranes and nerves, Proceedings of the National Academy of Sciences 102 (28) (2005) 9790–9795.

[11] A. J. Newton, R. A. McDougal, M. L. Hines, W. W. Lytton, Using neuron for reaction-diffusion modeling of extracellular dynamics, Frontiers in neuroinformatics 12 (2018) 41.

[12] H. C. Barron, Neural inhibition for continual learning and memory, Current opinion in neurobiology 67 (2021) 85–94.

[13] R. Follmann, E. Rosa Jr, W. Stein, Dynamics of signal propagation and collision in axons, Physical Review E 92 (3) (2015) 032707.

[14] E. P. Zemskov, M. A. Tsyganov, W. Horsthemke, Oscillatory multipulsons: Dissipative soliton trains in bistable reaction-diffusion systems with cross diffusion of attractive-repulsive type, Physical Review E 101 (3) (2020) 032208.

[15] E. P. Zemskov, A. Yu. Loskutov, Oscillatory traveling waves in excitable media, Journal of Experimental and Theoretical Physics 107 (2008) 344–349.

[16] E. P. Zemskov, A. Yu. Loskutov, Traveling waves in a piecewise-linear reaction-diffusion model of excitable medium, Biophysics 54 (2009) 631–636.

[17] P. K. Maini, Using mathematical models to help understand biological pattern formation, Comptes rendus. Biologies 327 (3) (2004) 225–234.

[18] B. Tabi Dzou, A. Etémé, A. Mvogo, C. Tabi, H. Ekobena Fouda, T. Kofané, Soliton-like nonlinear excitation in the FitzHugh–Nagumo cardiac model through the cubic–quintic complex Ginzburg–Landau equation, Nonlinear Dynamics (2024) 1–20.

[19] J. Rinzel, J. B. Keller, Traveling wave solutions of a nerve conduction equation, Biophysical journal 13 (12) (1973) 1313–1337.

[20] J. A. Feroe, Existence and stability of multiple impulse solutions of a nerve equation, SIAM Journal on Applied Mathematics 42 (2) (1982) 235–246.

[21] S. Das, M. Mukherjee, A. Mondal, K. C. Mistri, S. K. Mahato, M. Aziz-Alaoui, Traveling pulses and its wave solution scheme in a diffusively coupled 2D Hindmarsh-Rose excitable systems, Nonlinear Dynamics 111 (7) (2023) 6745–6755.

[22] H. L. Moreland, J. Dockery, Estimation of the traveling wave speed in pancreatic islets using high period periodic orbits, Applied Mathematics and Computation 439 (2023) 127482.

[23] S. P. Hastings, Single and multiple pulse waves for the FitzHugh-Nagumo, SIAM Journal on Applied Mathematics 42 (2) (1982) 247–260.

[24] E. P. Zemskov, K. Kassner, M. A. Tsyganov, M. J. B. Hauser, Wavy fronts in reaction-diffusion systems with cross advection, European Physical Journal B 72 (2009) 457–465.

[25] S. El-Wakil, M. Abdou, New explicit and exact traveling wave solutions for two nonlinear evolution equations, Nonlinear Dynamics 51 (2008) 585–594.

[26] P. T. Djomegni, K. Govinder, Generalized travelling wave solutions for hyperbolic chemotaxis PDEs, Applied Mathematical Modelling 40 (9-10) (2016) 5672–5688.

[27] N. Keerthana, R. Saranya, N. Annapoorani, Dynamics and diffusion limit of traveling waves in a two-species chemotactic model with logarithmic sensitivity, Mathematics and Computers in Simulation 222 (2024) 311–329.

[28] V. Mañosa, Periodic travelling waves in nonlinear reaction–diffusion equations via multiple Hopf bifurcation, Chaos, Solitons & Fractals 18 (2) (2003) 241–257.

[29] L. Chen, A. Jüngel, Analysis of a parabolic cross-diffusion population model without self-diffusion, Journal of Differential Equations 224 (1) (2006) 39–59.

[30] V. Méndez, W. Horsthemke, E. P. Zemskov, J. Casas-Vázquez, Segregation and pursuit waves in activator-inhibitor systems, Physical Review E 76 (4) (2007) 046222.

[31] V. K. Vanag, I. R. Epstein, Cross-diffusion and pattern formation in reaction–diffusion systems, Physical Chemistry Chemical Physics 11 (6) (2009) 897–912.

[32] B. Ermentrout, D. H. Terman, Foundations of mathematical neuroscience, Citeseer, 2010.

[33] E. P. Zemskov, I. R. Epstein, A. Muntean, Oscillatory pulses in FitzHugh-Nagumo type systems with cross-diffusion, Mathematical Medicine and Biology 28 (2) (2011) 217–226.

[34] M. Mansour, Traveling wave solutions of a nonlinear reaction–diffusion–chemotaxis model for bacterial pattern formation, Applied Mathematical Modelling 32 (2) (2008) 240–247.

[35] A. Mondal, A. Mondal, M. Aziz-Alaoui, R. K. Upadhyay, S. K. Sharma, C. G. Antonopoulos, The generation of diverse traveling pulses and its solution scheme in an excitable slow-fast dynamics, Chaos: An Interdisciplinary Journal of Nonlinear Science 32 (8) (2022).

[36] E. P. Zemskov, M. A. Tsyganov, W. Horsthemke, Oscillatory pulses and wave trains in a bistable reaction-diffusion system with cross diffusion, Physical Review E 95 (1) (2017) 012203.

[37] E. P. Zemskov, Wavy front dynamics in a three-component reaction-diffusion system with one activator and two inhibitors, Physical Review E 73 (4) (2006) 046127.

[38] H. Soleimani, A. Ahmadi, M. Bavandpour, Biologically inspired spiking neurons: Piecewise linear models and digital implementation, IEEE Transactions on Circuits and Systems I: Regular Papers 59 (12) (2012) 2991–3004.

[39] H. Soleimani, A. Ahmadi, M. Bavandpour, O. Sharifipoor, A generalized analog implementation of piecewise linear neuron models using ccii building blocks, Neural Networks 51 (2014) 26–38.

[40] Y. Zerlaut, S. Chemla, F. Chavane, A. Destexhe, Modeling mesoscopic cortical dynamics using a mean-field model of conductance-based networks of adaptive exponential integrate-and-fire neurons, Journal of computational neuroscience 44 (1) (2018) 45–61.

[41] S. Theodorakis, E. Svoukis, Piecewise linear emulation of propagating fronts as a method for determining their speeds, Physical Review E 68 (2) (2003) 027201.

[42] G. Cooper, K. Adams, The cell: a molecular approach, Oxford University Press, 2022.

[43] M. Sensi, M. Desroches, S. Rodrigues, Slow–fast dynamics in a neurotransmitter release model: Delayed response to a time-dependent input signal, Physica D: Nonlinear Phenomena 455 (2023) 133887.

[44] S.-L. Wu, W.-T. Li, Global asymptotic stability of bistable traveling fronts in reaction-diffusion systems and their applications to biological models, Chaos, Solitons & Fractals 40 (3) (2009) 1229–1239.

[45] M. Doumic, S. Hecht, B. Perthame, D. Peurichard, Multispecies cross-diffusions: from a nonlocal mean-field to a porous medium system without self-diffusion, Journal of Differential Equations 389 (2024) 228–256.

[46] E. P. Zemskov, I. R. Epstein, Wave propagation in a FitzHugh-Nagumo-type model with modified excitability, Physical Review E 82 (2) (2010) 026207.

[47] E. P. Zemskov, M. A. Tsyganov, K. Kassner, W. Horsthemke, Nonlinear waves in a quintic FitzHugh-Nagumo model with cross diffusion: Fronts, pulses, and wave trains, Chaos 31 (3) (2021) 033141.

[48] Y. Yu, Y. Shu, D. A. McCormick, Cortical action potential backpropagation explains spike threshold variability and rapid-onset kinetics, Journal of Neuroscience 28 (29) (2008) 7260–7272.

[49] P. A. Robinson, C. J. Rennie, J. J. Wright, Propagation and stability of waves of electrical activity in the cerebral cortex, Physical Review E 56 (1) (1997) 826.

[50] G. Lepeu, E. van Maren, K. Slabeva, C. Friedrichs-Maeder, M. Fuchs, W. J. Z'Graggen, C. Pollo, K. A. Schindler, A. Adamantidis, T. Proix, et al., The critical dynamics of hippocampal seizures, Nature Communications 15 (1) (2024) 6945.

[51] L. R. González-Ramírez, M. A. Kramer, The effect of inhibition on the existence of traveling wave solutions for a neural field model of human seizure termination, Journal of computational neuroscience 44 (2018) 393–409.

[52] J. D. Harris, B. Ermentrout, Traveling waves in a spatially-distributed wilson–cowan model of cortex: From fronts to pulses, Physica D: Nonlinear Phenomena 369 (2018) 30–46.